Equalization of Modal Dispersion in Multimode Fiber using Spatial Light Modulators

Elad Alon, Vladimir Stojanović, Joseph M. Kahn, Stephen Boyd, and Mark Horowitz
Department of Electrical Engineering, Stanford University, CA 94305, USA

***Abstract* – Intersymbol interference (ISI) due to modal dispersion is the dominant limitation to the bit rate-distance product in multimode fiber-optic communication systems. If the light launched into the fiber excites only the desired principal modes, modal dispersion can be eliminated. We can achieve this by using spatial light modulators (SLMs) to perform adaptive spatial filtering on the electric fields of the light. In this paper, we develop an optimization framework for setting the SLMs to obtain an upper bound on the achievable performance and develop heuristics that nearly reach this upper bound. Using this framework, we show that both a sophisticated semidefinite programming-based algorithm and a simple adaptive algorithm achieve performance close to the upper bound. Performance and system complexity tradeoff curves are constructed, showing that a 20×20 array of SLM pixels with binary phase control performs within 15% of more complex implementations. Finally, we extend the framework and present preliminary results showing the promise of further increases in the capabilities of multimode fiber by using the fiber as a multiple-input, multiple-output (MIMO) transmission medium.**

I. Introduction

Multimode fiber is the dominant type of fiber used for data communications in current local-area networks; these fibers have several non-idealities that limit the achievable signaling rates for a given length of fiber. The dominant limiting factor in multimode links is the ISI caused by modal dispersion [1].

Light can travel through a multimode fiber in many different modes; the modes in which light propagates depend upon the launch conditions at the input of the fiber. The existence of multiple modes makes multimode fiber easier to launch light into and therefore less expensive than single-mode fiber.

Since each of the modes propagates down the fiber with its own distinct group velocity, information carried by the modes arrives at the end of the fiber at different times. Therefore, an original pulse of data at the input of the fiber spreads apart into several pulses at the end of the fiber – otherwise known as modal dispersion. This effect is directly analogous to multi-path in wireless communication systems. At high data rates or on long fibers, the differences in arrival time of the various modes can span tens of symbols.

Electrical equalization [2,3] has been proposed and used to mitigate this potentially severe ISI. However, equalization in the electrical domain inherently amplifies the additive noise sources in the system (or attenuates the signal), leading to degradation of the achievable bit error rate [4].

Since the ISI at the receiver is a direct function of which modes are launched at the input of the fiber, we propose the use of SLMs to perform adaptive spatial filtering on the fields of the light such that only the desired modes are excited (Fig. 1). At the transmitter, a lens is used to perform a spatial Fourier transform on the transmitted electric field. An array of SLM pixels manipulates the phase and/or amplitude of the light in the spatial frequency domain, and reflects the modified light back to the same lens to perform the inverse Fourier transform. This approach is similar to the spatial filtering with computer-generated optical masks used by Dubois in [5]; however the use of SLMs allows the filtering to be adapted to an arbitrary, unknown fiber.

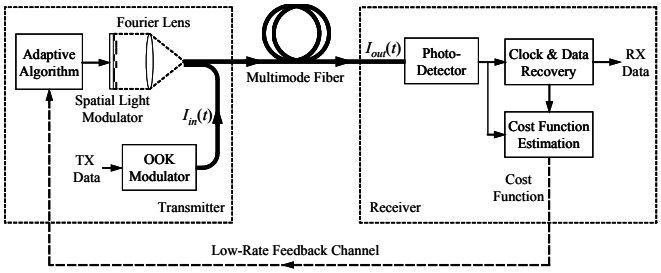

Fig. 1. Multimode fiber optic communication system using a spatial light modulator for adaptive spatial filtering.

Unlike traditional equalization, the energy of the light signal can literally be refocused into the desired modes of the fiber (eliminating the ISI) without amplifying the fixed noise in the system. Of course, this can only be achieved with the proper SLM pixel settings, and hence this paper addresses the task of optimizing these settings.

In order to develop an optimization framework, we first create a model of the optical fiber channel as a function of the SLM settings. Additionally, the passive nature of the SLMs introduces physical constraints that must be included in the optimization problem. Finally, to complete the optimization problem an appropriate objective function must be chosen, and we examine both the signal-to-interference ratio (SIR) and minimum distance between signal levels (d_{min}).

By deriving the dual of the optimization problem (which is guaranteed to be convex [6] even though the original problem is not), we can find provable upper bounds on the achievable performance for a given fiber and SLM system. Furthermore, the solution of the dual problem can be used in a heuristic to find solutions to the original problem.

In any real system, the modes and properties of the fiber may change with time (e.g. due to vibrations or temperature-induced geometric variations), making an adaptive algorithm for setting the SLM pixels highly desirable. Solving the dual optimization problem and using the resulting solution for heuristics involves a high level of computational complexity,

making this approach ill-suited to an adaptive solution. Therefore, we describe the single coordinate ascent algorithm [7] as an adaptive solution. Simulation results show that both the SLM settings generated by the computationally intensive heuristics and by single coordinate ascent very nearly achieve the performance upper bound.

This optimization framework allows us to explore tradeoffs between the performance and the complexity of the communication system. In addition, this same framework can be extended to explore further increases in the capacity of the multimode fiber by creating a MIMO system over a single multimode fiber, and we present preliminary results from this type of system showing the promise of this technique.

II. Channel Model and SLM Constraints

Multimode fibers are waveguides whose cores are large enough compared to the wavelength of the light that they support the existence of multiple distinct modes propagating at different group velocities. Ideally, these modes are orthogonal – in other words, energy launched in only one mode should remain in that mode when it exits the fiber. However, in all real fibers, these fundamental modes are coupled together as they propagate down the fiber due to bends and imperfections in the fiber fabrication [8]. Fortunately, even in the presence of these non-idealities which cause mode-mixing, the fiber will still have orthogonal principal modes with well-defined group delays [9].

In this work, we consider an ideal, weakly guiding step-index fiber, whose linearly polarized (LP) modes and their associated group delays are well-known in the literature [8] – spatial field patterns of two LP modes are shown in Fig. 2. Despite this simplified fiber (most deployed multimode fibers have graded-index profiles as well as mode-mixing), the optimization framework we consider is applicable to any fiber because it only relies on the modes of the fiber being orthogonal. Other optical non-idealities that are usually a concern in long-haul single-mode fiber (such as chromatic dispersion and polarization mode dispersion) are negligible in short multimode fibers, and therefore are not modeled in this work.

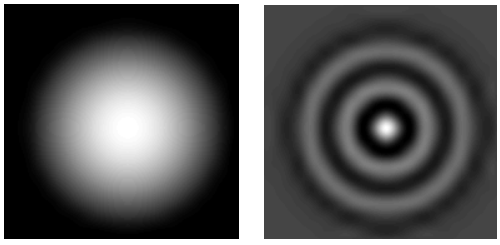

Fig. 2. Field patterns of two different modes in a 64 μm core 0.2% step-index fiber with an 850 nm laser.

Mathematically, the modes can be represented as a matrix ($\mathbf{\Psi}$) where each column of the matrix is a mode sampled in the spatial frequency domain. The SLM settings, a vector in spatial frequency[1] (x), set the field pattern of the light transmitted into the fiber. Since the modes of the fiber are orthogonal, the transmitted light can be decomposed onto the basis of the fiber modes by a matrix projection ($\mathbf{\Psi}^H x$). While this describes the portions of the electric field in each fiber mode, the receiver can only detect the field intensity. Therefore, the impulse response of the system as a function of the SLM settings is

$$I_{out}(\mathrm{t}) = x^H \mathbf{\Psi} \mathbf{F}(\mathrm{t}) \mathbf{\Psi}^H x, \tag{1}$$

where $\mathbf{F}(\mathrm{t})$ is a diagonal matrix containing impulses delayed by the propagation delays of the modes. It is important to note that since the SLM works in the electric field domain and the receiver detects intensity, the impulse response is a quadratic function of the SLM settings. The impulse response of an example fiber with the SLM set such that the light is focused at the center of the fiber is shown in Fig. 3.

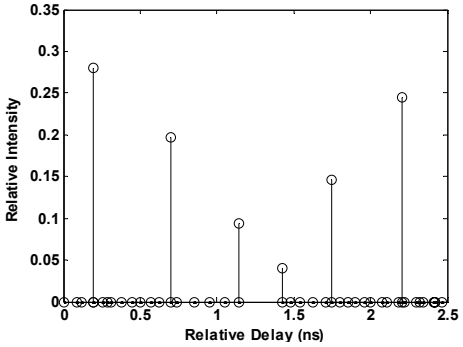

Fig. 3. Example pulse response for a 64 μm core 0.2% step-index fiber with an 850 nm laser focused in the center of the fiber.

Since the SLM is passive in nature, each component of x must be a complex number with magnitude less than or equal to one. In addition, most SLMs can affect only the magnitude or the phase of the incoming light signal, and often have limited precision in their settings. For example, if a Texas Instruments DLP mirror array [10] were used as the SLM, the SLM could only be set to either fully reflect the light onto the fiber (providing a magnitude of 1) or deflect the light away from the fiber (providing a magnitude of 0). For more general magnitude-only SLMs, each component of x must be a real number between zero and one. The constraints for phase-only SLMs are that each component of x is a complex number whose magnitude must be equal to one.

III. Optimization Framework and Analysis

With the channel model of the fiber and physical constraints of the SLMs in place, we can begin to construct the optimization framework. We first explore the choice of objective function, examining both a peak signal-to-interference ratio function and as well as the minimum margin between the two intensity levels. The dual of the optimization problem is then formulated to provide provable

[1] The two-dimensional array of pixels is transformed into a column vector to form x. The fiber modes are linearized in a similar fashion to construct $\mathbf{\Psi}$.

upper bounds on the achievable performance as well as intuition about solutions of the original problem.

A. Objective Function

Standard linear communication links are usually optimized based on some version of signal-to-interference ratio (SIR) or signal-to-interference-and-noise ratio (SINR). In our approach, the receiver detects intensity while the SLM acts on the electric field; therefore a standard SIR would be a ratio of 4th order polynomials, which is a very a difficult function to optimize. An objective function that can be reduced to a ratio of quadratic forms is SIR_{l1}, the peak SIR.

In order to calculate this cost function, only the symbol-spaced sampled pulse response of the system must be known. At a particular symbol rate, this pulse response can be calculated by summing together the intensities of the modes arriving at the end of the fiber within the same symbol interval. The group of modes (or single mode) which arrive together to form the highest intensity sample of the pulse response can be selected by an indicator diagonal matrix $\mathbf{I}_{\Delta main}$ (2a). All the remaining modes, which arrive in other symbol periods and cause ISI, can be selected by a second diagonal matrix $\mathbf{I}-\mathbf{I}_{\Delta main}$ (2b).

$$I_{out}^{main} = x^H \mathbf{\Psi} \mathbf{I}_{\Delta main} \mathbf{\Psi}^H x \tag{2a}$$

$$I_{out}^{ISI} = x^H \mathbf{\Psi} (\mathbf{I} - \mathbf{I}_{\Delta main}) \mathbf{\Psi}^H x \tag{2b}$$

The peak SIR is simply the ratio of I_{out}^{main} to I_{out}^{ISI}; this function resembles the standard SIR which can be used to minimize the bit error rate. Without constraints, the optimization problem with this objective function is

$$\underset{x}{\text{maximize}}\ \text{SIR}_{l1} = \frac{x^H \mathbf{\Psi} \mathbf{I}_{\Delta main} \mathbf{\Psi}^H x}{x^H \mathbf{\Psi} (\mathbf{I} - \mathbf{I}_{\Delta main}) \mathbf{\Psi}^H x}. \tag{3}$$

Even without constraints, this optimization problem is not convex. However, the objective function is a generalized Rayleigh quotient, which has a globally optimal solution corresponding to the generalized eigenvector with maximal generalized eigenvalue [11].

Unfortunately, the generalized eigenvector solution is not very energy efficient once it is scaled to meet the passivity constraints of the SLMs, and therefore does not perform very well in the presence of additive noise. In order to overcome this drawback, a noise term could be added to the denominator of (3), but adding the noise term causes the problem to no longer have a guaranteed optimum solution (since the Rayleigh quotient form is lost and the solution is no longer invariant to scaling).

An objective function that is proportional to the received intensity can be used to find energy-efficient SLM settings. Given that optical signals are often transmitted in binary NRZ format, we use an objective function that corresponds to the minimum distance between the received "0" and "1" symbols, d_{min}. The unconstrained optimization problem with d_{min} as the objective function becomes

$$\underset{x}{\text{maximize}}\ d_{min} = x^H \mathbf{P} x, \tag{4}$$

where we have defined $\mathbf{P} = \mathbf{\Psi}(2\mathbf{I}_{\Delta main} - \mathbf{I})\mathbf{\Psi}^H$.

Since the inner matrix $\mathbf{P}$ is never negative semidefinite, this maximization problem is clearly non-convex, but it does have a global solution, as do all unconstrained quadratic optimization problems [6]. However, the global solution property is once again lost when the passivity constraints of the SLMs are included (5); therefore heuristics will need to be used to solve this optimization problem.

$$\begin{aligned} &\text{maximize} && x^H \mathbf{P} x \\ &\text{subject to} && |x_k| \le 1, k = 1, ..., N, x \in C^N \end{aligned} \tag{5}$$

B. Dual Problem Formulation

In order to guide the development of these heuristics and obtain bounds on the achievable d_{min}, we formulate the dual of problem (5). The first step to construct the dual problem is to form the Lagrangian, which for problem (5) is

$$L(x,\lambda) = x^H \left(\mathbf{P} + \text{diag}(\lambda)\right) x - \lambda^T \mathbf{1}, \tag{6}$$

where λ is the dual variable.

Before proceeding with the formulation of the dual problem, we examine one of the optimality conditions implied by the Lagrangian because it leads to an interesting insight about optimal SLM settings.

$$\frac{\partial L(x,\lambda)}{\partial \lambda} = \text{diag}(x^H) x - \mathbf{1} = 0 \tag{7}$$

Equation (7) implies that each of the components of an optimal x will have a magnitude equal to one. In other words, at the optimal setting, the SLM will modify only the phase (and not the magnitude) of the light in the spatial frequency domain. Intuitively, this result should not be unexpected because d_{min} is proportional to the magnitude of the input signal, and the magnitude of the input signal is maximized when the SLM is purely reflective.

Since an SLM that could modulate both phase and magnitude would modify only phase at an optimal setting, the optimization problem with only the passivity constraint (5) is actually equivalent to an optimization problem with a phase-only constraint ($|x_k|=1$). The dual of both of these optimization problems is

$$\begin{aligned} &\text{minimize} && \mathbf{1}^T \lambda \\ &\text{subject to} && \mathbf{P} + \text{diag}(\lambda) \ge 0 \\ & && \lambda \ge 0 \end{aligned} \tag{8}$$

This problem is a standard semidefinite program (SDP), and can be solved straightforwardly (but with high computational intensity) using an interior point method [6].

The optimal value of the objective function in (8) provides an upper bound on the achievable minimum distance. This upper bound is a key result of the optimization analysis that will be used as a metric in developing efficient heuristics presented in the rest of the paper.

IV. Optimization Algorithms

In order to recover more direct information to assist us in finding solutions to the original problem, it is useful to find the dual of the dual problem (8), which is the SDP:

$$\begin{aligned} &\text{maximize} && \mathrm{Tr}(\mathbf{PX}) \\ &\text{subject to} && \mathbf{X} \geq 0 \\ & && \mathbf{X}_{ii} = 1 \end{aligned} \tag{9}$$

Both (8) and (9) are well-known problems because they appear as duals of the two-way partitioning problem [6], whose cost function is identical in form to that of (5), but where the constraints are replaced with binary component-wise equality constraints ($x_i^2=1$). In that context, one of the interpretations of the dual variable $\mathbf{X}$ is that it represents a covariance matrix of the original variable x; it provides information about a probability distribution that can be used to generate potential solutions to the original problem.

In the two-way partitioning problem, a well-known heuristic algorithm involves generating a set of random vectors x' from a multivariate, zero-mean normal distribution with covariance $\mathbf{X}$. Each x' is converted to a valid solution of the problem by taking the sign of each of the individual components, and then the solution that achieves the highest objective function is chosen.

Unlike the two-way partitioning problem, the variables in (5) are complex-valued, and therefore it is not immediately clear how to apply the covariance matrix $\mathbf{X}$ to generate random complex numbers with unit magnitudes. We therefore describe an extension to the SDP-based heuristic algorithm used in the two-way partitioning problem. This heuristic has high computational complexity and assumes knowledge of the channel, so following the SDP-based heuristic we describe the single coordinate ascent algorithm which is well-suited to an adaptive hardware implementation.

A. SDP-based Heuristic

In order to extend the two-way partitioning heuristic, we first revisit the objective function in (5) by splitting x into its real and imaginary components x_R and x_I.

$$(x_R + jx_I)^H \mathbf{P}(x_R + jx_I) = x_R{}^H \mathbf{P} x_R + x_I{}^H \mathbf{P} x_I \tag{10}$$

As clearly shown by (10), the objective function is separable in the real and imaginary components of x, and therefore (5) can be rewritten as

$$\begin{aligned} &\text{maximize} && z^{\mathrm{T}} \begin{bmatrix} \mathbf{P} & \mathbf{0} \\ \mathbf{0} & \mathbf{P} \end{bmatrix} z \\ &\text{subject to} && z_k{}^2 + z_{k+N}{}^2 \leq 1, k = 1, \ldots, N, z \in \mathbb{R}^{2N} \end{aligned} \tag{11}$$

where $z^{\mathrm{T}} = [x_R{}^{\mathrm{T}}\ x_I{}^{\mathrm{T}}]$. The dual of (11) is identical to (8) but with the positive semidefinite constraint repeated twice. Leaving the redundant constraint in the dual of (11) and forming the dual once more leads to the covariance matrix

$$\mathbf{Z} = \begin{bmatrix} \mathbf{X} & \mathbf{0} \\ \mathbf{0} & \mathbf{X} \end{bmatrix}. \tag{12}$$

Clearly, the interpretation of $\mathbf{Z}$ is that the original covariance matrix $\mathbf{X}$ obtained by solving (9) can be used to generate a set of pairs of random vectors (x_R' and x_I') which are independent, identically distributed. To create valid solutions for (5) from these vectors, each component of the vector defined by $x_R' + jx_I'$ is rescaled such that its magnitude is equal to one (i.e. the angle information is preserved); to complete the heuristic we simply choose the solution that achieves the highest d_{min}.

As the results in the next section show, this heuristic algorithm finds solutions that very nearly achieve the upper bound on d_{min} calculated from solving (8). However, the algorithm involves a high degree of computation (solving an SDP and then generating a large number of samples from a random distribution) and, in addition, it assumes knowledge of the field patterns of the modes of the fiber.

B. Single Coordinate Ascent

One of the simplest optimization algorithms (both in terms of computational complexity and hardware implementation) is single coordinate ascent (SCA) [7]. At each step of the SCA algorithm, all of the variables in the problem are fixed except for one. The current variable (which in this case is the angle of the kth component of x, θ_k) is perturbed in the positive and negative directions by a small step ($\Delta\theta$) and the objective function is measured at all three possible settings (θ_k, $\theta_k+\Delta\theta$, and $\theta_k-\Delta\theta$). The algorithm then simply picks the setting with the highest objective function and moves on to the next variable.

This algorithm can be applied with any initial condition, but since the problem is non-convex the algorithm may converge to different solutions with different initial settings. In particular, the algorithm can be applied to the solution generated by the SDP-based heuristic to improve its performance even further. Another initial condition of interest for this algorithm is the default setting of the SLMs which focuses the light onto the center of the fiber.

SCA is ideally suited to an adaptive solution because of its low complexity. The hardware need only have the capability to measure (or estimate) the objective function d_{min} at the receiver and increment or decrement the variable settings. Measurement of d_{min} can be accomplished by adding to the receiver a secondary slicer with an adjustable threshold set by a tracking loop (Fig. 4).

For each new SLM setting, d_{min} is measured in the following manner; first, the tracking algorithm resets the threshold of the error sampler to the highest possible level.

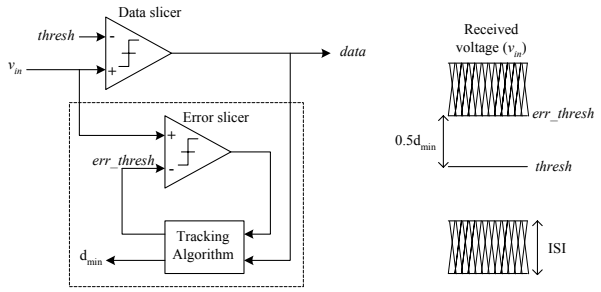

Fig. 4. Additional error slicer and tracking algorithm hardware in the receiver to enable measurement of d_{min}.

Each time the error slicer indicates that the input data was below its threshold and the data slicer indicates that the input data was above its threshold, the tracking algorithm lowers *err_thresh* by a small amount (e.g. by subtracting 1 LSB from the control code of the DAC that generates *err_thresh*). At some point, the algorithm reaches a point where no received 1's lie below *err_thresh*; d_{min} can then be calculated from *thresh* and *err_thresh*, as shown in Fig. 4[2]. The hardware can detect that it has reached this point by waiting for a period of many consecutive bits in which *err_thresh* was not adjusted downwards. Another option involves simply running the tracking algorithm over a fixed number of received bits and then estimating d_{min} from the final *err_thresh*.

Clearly, negative values of d_{min} cannot be correctly measured by this algorithm. If the eye is closed with the initial SLM settings, known training patterns (e.g. a single pulse response) can be used to simplify the measurement of d_{min}. SCA can then be applied to open the eye so that d_{min} can be measured from live data.

Even if the eye is open, the finite window over which d_{min} is measured, additive noise, and quantization in the measurement will result in errors in the estimated margin. In order to explore the ideal capabilities of SCA, we will assume that these effects are negligible in the rest of this paper.

V. Simulation Results

In this section we will first provide insight into the mechanism by which an SLM compensates for modal dispersion. We will then explore the performance of the above algorithms as a function of the system complexity.

A. Fiber and System Parameters

To calculate the spatial field patterns of the modes ($\boldsymbol{\Psi}$) and their associated group delays, we assume 1km of weakly guiding multimode fiber with a 0.2% step index profile and a 64 μm core. The target data rate is 10 Gb/s at a wavelength of 850 nm.

Ignoring the polarization degree of freedom, there are 88 total modes in this fiber. As shown in Fig. 5, the differences between the group delays of the modes spread over 25 symbol intervals at 10 Gb/s.

[2] This algorithm can be extended to deal with nonlinearities by calculating the distance between the minimum high and maximum low levels.

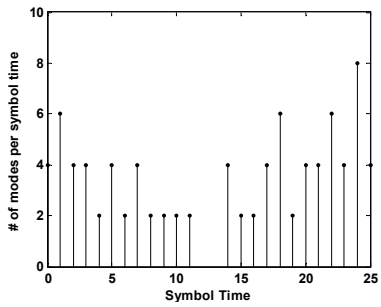

Fig. 5. Number of modes per symbol time at 10 Gb/s for a 0.2% step-index fiber with 64 μm core and an 850 nm laser. There are 88 total modes.

Unless otherwise noted, we will use a phase-only SLM for the rest of this paper. For the purposes of the following example, we use a 400-pixel SLM (in a 20×20 array) with 1° of phase resolution.

B. Example Optimization Results

The first optimization procedure uses only the SDP-based heuristic, whereas the second procedure applies SCA to the solution generated by the first procedure. The third procedure uses SCA starting from an initial SLM setting in which the light is focused in the center of the fiber.

The impacts of the three optimizations on the pulse response at 10 Gb/s are shown in Fig. 6. There are several important points to notice from these responses. First, severe ISI is present in the un-optimized pulse response of Fig. 6(a), whereas ISI is almost completely absent in all three of the optimized pulse responses. Additionally, all three procedures have actually refocused the energy of the transmitted light into a useful mode as opposed to simply canceling the ISI.

The upper bound on d_{min} is 0.984, and all three procedures achieve a value within 7% of this bound, proving that these algorithms are all capable of generating extremely good solutions. The difference between the performance achieved by SCA alone and the performance achieved by the SDP heuristic followed by SCA is negligible. This is encouraging

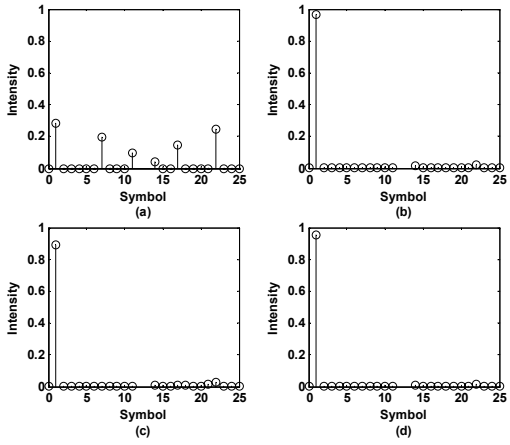

Fig. 6. Pulse responses for (a) SLM set to focus in the center of the fiber. (b) SCA applied to the focused setting. (c) SDP-based heuristic. (d) SCA applied to SDP-based heuristic solution. The intensities have been normalized to the total intensity present in the original pulse response of (a).

because it means that an adaptive system based on SCA can achieve a d_{min} comparable to that of much more sophisticated (and difficult to implement) algorithms.

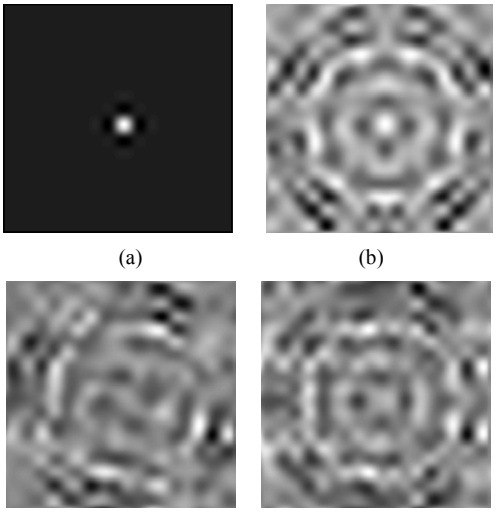

(a) (b)

(c) (d)

Fig. 7. Field patterns for (a) SLM set to focus in the center of the fiber. (b) SCA applied to the focused setting. (c) SDP-based heuristic. (d) SCA applied to SDP-based heuristic solution.

The field patterns chosen by the three optimization procedures are shown alongside the focused setting in Fig. 7. Interestingly, despite the fact that the pulse responses of all three optimized settings look very similar, the actual field patterns at the input of the fiber are somewhat different. This can be explained by the fact that the algorithms are free to choose a linear combination of the modes that arrive within the same symbol time, and therefore there can be a high degree of flexibility in the actual choice of field pattern.

C. Performance and System Complexity Tradeoffs

Using the optimization framework we have developed, we proceed to explore the performance of the algorithms as we vary the complexity of the system. The first parameter we examine is the number of pixels in the SLM. The size of the SLM array sets the spatial resolution of the field pattern imaged onto the input of the fiber – a larger array achieves higher resolution. As shown in Fig. 8, the performance returns diminish very quickly past an array of size of roughly 400 pixels. Intuitively, this can be explained by the fact that once the system has achieved high enough spatial resolution that the field pattern is roughly constant over the entire pixel, further increases in the resolution do not drastically alter the image generated by the SLMs, and therefore the performance of the equalization remains roughly constant.

The other important point to notice from Fig. 8 is that across the entire range of array sizes for which SDP-based optimizations were performed, SCA alone achieved nearly equivalent d_{min} – the three curves are nearly indistinguishable. Since the optimization problem is non-convex, there is no guarantee that this phenomenon will hold true for all fibers and/or systems, but it is nonetheless encouraging that for all

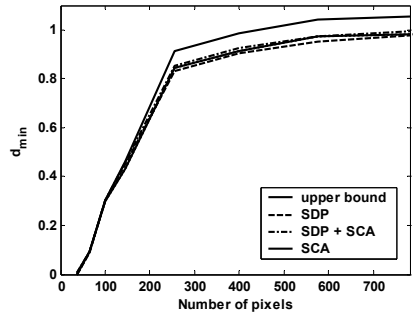

Fig. 8. Performance (d_{min}) versus number of pixels for an SLM with 1° of phase resolution.

the optimizations we have run, SCA performs extremely well.

Another parameter of interest is the phase quantization of the SLM, since it drives the complexity of the electronics that control the pixels in the array. Having concluded from Fig. 8 that an array of 400 pixels can achieve performance comparable to that of much larger arrays, we show in Fig. 9 the performance of an array of this size versus the phase resolution of the SLM. While performance generally increases with higher resolution, binary phase SLMs achieve a d_{min} within 10% of the d_{min} achieved with 1° resolution.

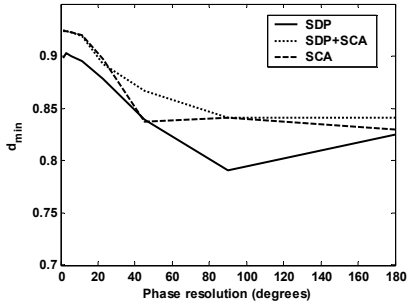

Fig. 9. Performance (d_{min}) versus phase resolution for a 400-pixel SLM.

Based on the curves shown in Figs. 8 and 9, a 20×20 binary phase SLM appears to be an attractive point in the tradeoff space between system complexity and performance.

VI. MIMO OVER MULTIMODE FIBER

The orthogonality of the principal modes of a multimode fiber can further be exploited to create multiple communication channels over a single multimode fiber [12]. Unlike the single channel system described so far, in order to achieve this MIMO system spatial filtering for each channel must be performed at both the transmitter (to selectively excite the modes assigned to a particular channel) and at the receiver (to filter out light from the other channels). For this initial exploration, we will assume that each channel has its own transmitter with associated SLM, and that the light from the *N* parallel channels can be combined into the fiber without incurring any loss. Similarly, we assume that the demultiplexing of the received light onto the *N* parallel SLMs is lossless. Finally, we assume that modes have been assigned to the channels *a priori*. This final assumption simplifies the simulations so that the basic characteristics of MIMO systems can be explored. In actual implementations,

the system will need to employ initialization algorithms to guarantee that each channel picks a different set of modes.

The system's impulse response must be extended to include the spatial filtering performed by the receive SLMs of each channel. In addition, light from one channel that is unfiltered by the receive SLMs of the other channels will cause inter-channel interference (ICI). Incorporating these effects, the impulse response from transmitter *j* to receiver *i* is

$$I_{out_{ij}}(\mathrm{t}) = m_{ij}{}^{H}\mathbf{F}(\mathrm{t})m_{ij}, \tag{13}$$

where we have defined $m_{ij} = \mathrm{diag}\left(\mathbf{\Psi}^{H} x_i^{rx}\right) \cdot \mathbf{\Psi}^{H} x_j^{tx}$.

The minimum margin of each channel ($\mathrm{d}_{\mathrm{min}_i}$) is set by both the self-induced ISI and the ICI caused by all of the other channels. For example, in a two-channel MIMO system,

$$\mathrm{d}_{\mathrm{min}_1} = \begin{bmatrix} m_{11}{}^{H} & m_{12}{}^{H} \end{bmatrix} \begin{bmatrix} 2\mathbf{I}_{\Delta main_1} - \mathbf{I} & \mathbf{0} \\ \mathbf{0} & -\mathbf{I} \end{bmatrix} \begin{bmatrix} m_{11} \\ m_{12} \end{bmatrix}. \tag{14}$$

There are several different methods to combine the margins of each channel to construct a single objective function for the optimization. We will assume that the data rate on the *N* channels are identical and are dictated by the achievable rate on the worst channel, and therefore we choose *min* $\{\mathrm{d}_{\mathrm{min}_i}, i = 1,\ldots,N\}$ as the objective function.

Using this objective function, SCA was performed on a example two-channel system, and the optimized pulse responses are shown in Fig. 10. The optimization was very successful in minimizing both ISI and ICI. The slight loss in pulse amplitude as compared to the SISO system is due to the addition of the SLMs at the receiver – the MIMO system has two cascaded spatial filters (with efficiencies < 1), as compared to the single SLM used in the SISO system.

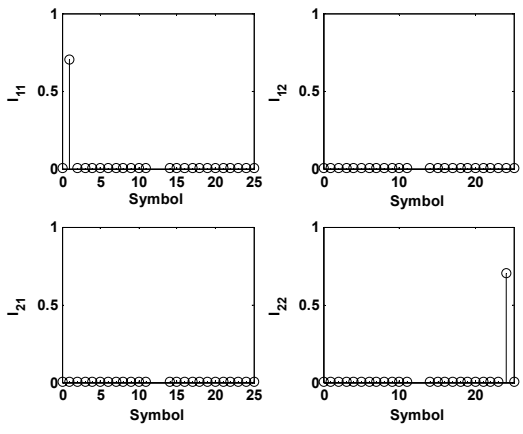

Fig. 10. Optimized pulse responses for a two-channel MIMO system at 10 Gb/s per channel over 1 km of a single multimode fiber. Each channel has a 20×20 binary phase SLM at both the transmitter and the receiver.

VI. Conclusion

We have developed an optimization framework for analyzing the use of SLMs to equalize modal dispersion in communication links on multimode optical fiber. SLM settings which literally refocus the transmitted energy into the desired modes can be found using either a sophisticated, SDP-based heuristic, or a simple SCA algorithm with nearly identical performance. The dual optimization problem was constructed to provide upper bounds against which to compare the performance achieved by these algorithms.

Exploration of the tradeoffs between the complexity of the system and the achievable performance indicates that a 400-pixel SLM with binary phase control performs equalization of modal dispersion nearly as effectively as much more complicated systems. In addition, preliminary results show that a MIMO system can effectively exploit modal diversity to create orthogonal communication channels over a single multimode fiber.

Spatial filtering based on SLMs is a very promising approach to greatly increase the data-carrying capability of widely installed multimode fibers. There is still a large amount of research to be done in the modeling of multimode fiber, in particular the time-varying properties of mode mixing and the associated changes in the principle modes. In addition to further exploring this area from a theoretical and simulation perspective, we are actively engaged in building a hardware implementation of the SLM-based multimode fiber communication system.

Acknowledgements

The authors wish to acknowledge the help of Z.-Q. Luo of the University of Minnesota in constructing the optimization framework, and O. Solgaard and S. Fan of Stanford University for useful discussions. J. M. Kahn is grateful for an IBM Faculty Award. E. Alon and V. Stojanović also thank M. Lee and I. Stojanović for their support.

References

[1] G. P. Agarwal, *Fiber-Optic Communication Systems*, Third Edition, Wiley, 2002.

[2] X. Zhao and F. S. Choa, "Demonstration of 10-Gb/s transmissions over 1.5-km-long multimode fiber using equalization techniques," *IEEE Photonics Technology Letters*, vol. 14, no. 8, pp. 1187-1189, Aug. 2002.

[3] H. Wu, J. A. Tierno, P. Pepeljugoski, J. Schaub, S. Gowda, J. A. Kash, and A. Hajimiri, "Integrated transversal equalizers in high-speed fiber-optic systems," *IEEE J. Solid-State Circuits*, vol. 38, pp. 2131-2137, Dec. 2003.

[4] J. Proakis, *Digital Communications*, Fourth Edition, McGraw-Hill, 2001.

[5] F. Dubois, Ph. Emplit, and O. Hugon, "Selective mode excitation in graded-index multimode fiber by a computer-generated optical mask," *Optics Letters*, vol. 19, no. 7, pp. 433-435, April 1994.

[6] S. Boyd and L. Vandenberghe, *Convex Optimization*, Cambridge University Press, 2003.

[7] I. Sharfer and A. O. Hero III, "A maximum likelihood digital receiver using coordinate ascent and the discrete wavelet transform," *IEEE Transactions on Signal Processing*, vol. 47, no. 3, pp. 813-825, March 1999.

[8] D. Marcuse, *Theory of Dielectric Optical Waveguides*, Elsevier Science & Technology Books, 1991.

[9] S. Fan and J. M. Kahn, "Principal modes in multi-mode waveguides", to be published in *Optics Letters*.

[10] P. F. Van Kessel, L. J. Hornbeck, R. E. Meier, and M. R. Douglass, "A MEMS-based projection display," *Proceedings of the IEEE*, vol. 86, no. 8, pp. 1687-1704, Aug. 1998.

[11] G. H. Golub and C. F. V. Loan, *Matrix Computations,* The Johns Hopkins University Press, 1996.

[12] H. R. Stuart, "Dispersive multiplexing in multimode optical fiber," *Science*, vol. 289, pp. 281-283, July 2000.